ORIGINAL ARTICLE

Predicting nickel resources recoverable potential and their uncertainty in a sector of *San Felipe* deposit

Predicción del potencial recuperable de recursos niquelíferos y su incertidumbre en un sector del depósito *San Felipe*

José Alberto Arias-del Toro[1], Alain Carballo-Peña[2*], Elmidio Estévez-Cruz[3], Rosa María Cobas-Botey[1]

[1]National Enterprise of Mineral Resources, Havana, Cuba.

[2]University of Moa, Holguín, Cuba.

[3]University of Pinar del Río, Pinar del Río, Cuba.

[*]Corresponding author: acarballo@ismm.edu.cu

Abstract

Estimation of recoverable resources is closely linked to mining selective and its primary objective is maximizing the profit from exploitation. Since estimation models inevitably suffer from the "softening" effect of the estimated law, they are inappropriate for predicting both the law and the tonnage of resources that could be recovered. Conversely, useful mineral law models obtained from applying geostatistical simulation efficiently reproduce global characteristics (texture), statistics (histogram) and spatial variability (variogram). Recoverable resource potential was predicted by applying sequential simulation method for 25m x 25m x 1m tonnage panel, metal quantity, mean grade and associated uncertainties, through a change of support and by applying several laws of cut in a small sector of San Felipe nickel deposit, chosen as a case study. In conclusion, changing the cut-off law over a given estimated medium has an effect on recoverable resources: as the cut-off law increases, tonnage and metal quantity decrease; conversely, the average nickel law increases, but uncertainty increases in all cases, due to the growth of average estimation errors associated with each of these parameters.

Keywords: recoverable resources, change of support, sequential Gaussian simulation method, uncertainty

Resumen

La estimación de los recursos recuperables se vincula estrechamente con la selectividad minera, su objetivo primordial es maximizar el beneficio de la

explotación. Dado que los modelos de estimación sufren inevitablemente el efecto de "suavizamiento" de la ley estimada, resultan inapropiados para predecir tanto la ley como el tonelaje de los recursos que pudieran ser recuperados. Contrariamente, los modelos de la ley del mineral útil obtenidos de la aplicación de la simulación geoestadística reproducen satisfactoriamente las características globales (la textura), la estadística (histograma) y variabilidad espacial (variograma). Mediante la aplicación del método de simulación secuencial gaussiana se simuló la ley de níquel en una densa red de puntos de 12,5 m x 12,5 m x 1 m para 100 escenarios equiprobables. Posteriormente, se realizó la predicción del potencial de recursos recuperables para el panel de 25 m x 25 m x 1 m del tonelaje, la cantidad de metal, la ley media y las incertidumbres asociadas, a través de un cambio de soporte y la aplicación de varias leyes de corte en un pequeño sector del depósito niquelífero San Felipe, escogido como caso de estudio. Se concluye que al variar la ley de corte sobre un determinado soporte de estimación se produce un efecto en los recursos recuperables: a medida que se incrementa la ley de corte, el tonelaje y la cantidad de metal disminuyen; contrariamente, la ley media de níquel se incrementa, pero la incertidumbre se incrementa en todos los casos, debido al incremento de los errores medios de estimación asociados a cada uno de estos parámetros.

Palabras clave: recursos recuperables, cambio de soporte, simulación secuencial gaussiana, incertidumbre

1. INTRODUCTION

The estimation of recoverable resources is closely linked to mining selectivity, the primary goal of which is to maximize exploitation profit; its difficulty lies in accurately predicting the characteristics of the *in situ* ore, considering that selection is performed on a certain volume and not punctually on drill holes (Chica-Olmo, 1987).

Changing the estimation support means discretizing the volume or support (panel) in which the parameters will be estimated into smaller units, in order to predict the grade distribution at a volume equivalent to the size of the Selective Mining Unit (SMU), given the grade distribution of the samples (point data).

The Selective Mining Unit (SMU) constitutes the smallest volume of material that can be selectively extracted, whether ore or waste, the dimensions of which will be conditioned by the mining method and the mining equipment utilized (Neufeld and Leuangthong, 2005; Sinclair and Blackwell, 2006; Rossi and Deutsch, 2014).

The grade smoothing effect, as a consequence of using estimators, is always present, especially when estimation is performed from widely spaced data.

The discrepancy between the distribution of the estimated grade and the grade distribution of the selective mining units is termed conditional bias. This occurs when the expected value of the true ore grade ($Z_v^* = z$) conditioned on the estimated grade $E\{Z_v|Z_v^* = z\} \neq z$ is not equal to the estimated grade $\{Z_v|Z_v^* = z\} \neq z$, where v represents the estimation volume (Rossi and Deutsch, 2014).

Unlike estimation, conditional simulation produces models of the variable of interest where global characteristics (texture), statistics (histogram), and spatial variability (variogram) are reproduced, providing alternative global representations where patterns of spatial continuity reproduction prevail. This allows for the construction of equiprobable numerical models of the variable in question.

The use of the conditional simulation technique enables the change of support. Its principle is based on simulating point values of the grade at the scale of smaller blocks and averaging the obtained values within the panel to obtain the grade value in a given equiprobable simulated scenario. The panel estimate and its uncertainty will result from the average of a series of *n* conditional simulations.

The objective of the present study was to predict the global recoverable resource potential from the nickeliferous mineralization contained in the weathering horizons and to quantify its uncertainty for various nickel cut-off grade values. For this purpose, 25 m x 25 m x 1 m panels were used within the limits of the studied sector of the San Felipe nickel deposit, starting from the simulated nickel grade at a point scale for 100 equiprobable scenarios, and through the use of the Sequential Gaussian Simulation technique.

Geology of the Study Sector The study sector is located in an area of the southeastern portion of the San Felipe nickel deposit, in the Cuban province of Camagüey. A weathering crust of the linear mantle type, of Tertiary age (Cobas-Botey et al., 2017) and with high silica content (Chang-Rodríguez and Rojas-Purón, 2018), develops over this area. It is formed from ultramafic rocks, mainly serpentinized harzburgites, where subordinate mafic cumulates, parallel diabase dikes, and oceanic basalts also appear (Rodríguez-Catalá and Rodríguez-Infante, 2021).

The nickel ore is essentially of silicated smectitic clay composition (nontronite and montmorillonite), also referred to as clay-type (Gallardo et al., 2010; Cobas-Botey et al., 2017). The mineral appears in the form of iron oxides and

hydroxides, with nickel concentrated as inclusions within aluminosilicates (clays) and magnesium silicates (serpentine), and to a lesser extent, associated with chromites and manganese oxides, distributed regularly and continuously throughout the deposit (Cobas-Botey, 2017).

The profile of the weathering crust developed in the San Felipe nickel deposit presents a transitional lithological zonation at depth, formed by six horizons (Cobas-Botey, 2017). For geostatistical modeling in the present study, the horizons of non-textural ochres with pisolites (ONTCP) and non-textural ochres without pisolites (ONT) are considered as a single unit: non-textural ochres (ONT). The rest of the weathering crust horizons remain as described by Cobas-Botey (2017).

2. MATERIALS AND METHODS

2.1. Database of the Study Sector

The database of the studied sector used for this research is composed of 4,113 composites of one-meter length, where each composite possesses the nickel content and the lithological code of the corresponding weathering horizon. The data come from 181 vertical wells with an average depth of 24.5 m, drilled in a 100 m x 100 m exploration grid, where wells appear locally in a 25 m x 25 m grid, as well as others arranged radially, spaced at smaller distances of approximately 12.5 m.

2.1.1 Volumetric Density

The volumetric density (Table 1) was obtained by averaging the dry density values of each weathering horizon. These values were transferred to the 25m x 25 m x 1 m panels to obtain the recoverable resources.

Table 1. Average dry volumetric density by weathering horizons

Weathering Horizon	Average Dry Volumetric Density (t/m³)
Non-Textural Ochres (ONT)	1,68
Limonitic Textural Ochres (OTL)	1,24
Saprolitic Textural Ochres (OTS)	1,09
Nontronized Serpentinites (SN)	0,96
Leached Serpentinites (SL)	1,05

The database of the studied sector used for this research is composed of 4,113 composites of one-meter length, where each composite possesses

the nickel content and the lithological code of the corresponding weathering horizon. The data come from 181 vertical wells with an average depth of 24.5 m, drilled in a 100 m x 100 m exploration grid, where wells appear locally in a 25 m x 25 m grid, as well as others arranged radially, spaced at smaller distances of approximately 12.5 m.

2.2. Procedure for Determining Recoverable Resources and Quantifying Associated Uncertainty

Based on the geological characteristics of the San Felipe nickel deposit, the determination of recoverable resources and the quantification of their uncertainty in the sector under study was carried out in the following stages:

Stage 1. Data Pre-processing

Validation of the database and creation of composites. Unfolding of composites with reference to the Digital Elevation Model (DEM) (Richmond, 2013). Exploratory Data Analysis. Detection of outliers, capping via accumulated metal curves (Equation 1). Boundary analysis between weathering horizons (Sterk et al., 2019; Kapageridis et al., 2021). Declustering into 100 m x 100 m cells.

$$\text{Accumulated metal} = \sum_{K=1}^{n} n_k \cdot \bar{C}_k \quad (1)$$

Where: n_k is the quantity of composites whose content lies within the k-th percentile interval of the nickel grade statistical distribution, and $\bar{C}_k$ is the mean nickel grade of the k-th interval.

Stage 2. Geostatistical Transformation

Gaussian transformation of nickel composites, conditioned to weathering horizons using the Normal Scores method from GSLIB (Deutsch and Journel, 1998).

Stage 3. Structural Analysis

Calculation and fitting of global directional experimental semi-variograms of the conditionally Gaussian-transformed nickel composites. Verification of the predictability of the fitted theoretical model via cross-validation (Webster and Oliver, 2007).

Stage 4. Simulation and Validation

Sequential Gaussian Simulation on a grid of nodes of 12.5 m x 12.5 m x 1 m for 100 equiprobable scenarios, using the SGSIM algorithm (Remy, Boucher, and Wu, 2009). Back-transformation of simulated Gaussian nickel values to

real nickel values (BACKTR procedure from GSLIB (Deutsch and Journel, 1998)). Validation of simulated scenarios (checking reproducibility of histograms and global variograms).

Stage 5. Change of Support

Change of support by scaling (Neufeld and Leuangthong, 2005) of the nickel grade to a panel of dimensions 25 m x 25 m x 1 m. Determination of tonnage $t(u_i; z_c)$, metal quantity $q(u_i; z_c)$ and mean grade $m(u_i; z_c)$, from the simulated *values using* cut-off values between 0% and 2.5% nickel, according to the indicator function: If $Z_v(u_i) \geq Z_c$ then $I_v(u_i; z_c) = 1$, 0 $otherwise$, and equations 2, 3 y 4:

$$t(u_i; z_c) = \quad I_v(u_i; z_c).p(u_i; z_c).v_{usm}.\bar{d}_h \tag{2}$$

$$q(u_i; z_c) = \quad I_v(u_i; z_c).Z_p(u_i; z_c).v_{usm}.\bar{d}_h \tag{3}$$

$$m(u_i; z_c) = \quad q(u_i; z_c)/t(u_i; z_c) \tag{4}$$

Where: $\bar{d}_h =$ mean density of the horizon in t/m^3, $.v_{usm}$ volume of the USM with dimensions of 12.5 m x 12.5 m x 1 m, igual a 156.25 m^3.

Stage 6. Recoverable Resources

Computation of mean values and their associated conditional variances, by cut-off grade, for tonnage (T_{z_c}), metal quantity (Q_{z_c}), recoverable mean nickel grade (M_{z_c}), and mineral probability P_{z_c}, in each 25 m x 25 m x 1 m panel, for the 100 simulated equiprobable scenarios, according to the condition $m(u_i; z_c) , \geq z_c$ (equations 5, 6, 7 y 8):

$$T_{z_c} = \frac{1}{N}\sum_{i=1}^{100} t(u_i; z_c) \tag{5}$$

$$Q_{z_c} = \frac{1}{N}\sum_{i=1}^{100} m.t(u_i; z_c) \tag{6}$$

$$M_{z_c} = \frac{1}{N}\sum_{i=1}^{100} \frac{Q_{z_c}}{T_{z_c}} \tag{7}$$

$$P_{z_c} = \frac{1}{N}\sum_{i=1}^{100} n(u_i; z_c) \tag{8}$$

Stage 7. Uncertainty Quantification

Quantification of the uncertainty of parameters T_{z_c}, Q_{z_c} and M_{z_c} through confidence intervals IC_{z_c} (Yamamoto, 1999; Murphy *et al.*, 2005; Artica, 2023) based on the calculation of error E_{z_c}(equations 9 y 10):

$$E_{z_c} = t.\frac{\sigma_{z_c}}{\sqrt{n_{z_c}}} \quad (9)$$

$$IC_{z_c} = M_{z_c} \pm \ E_{z_c} \quad (10)$$

Where t is the Student's t-value with $n_{z_c} - 1$ degrees of freedom for a 95% probability, σ_{z_c} - is the standard deviation obtained from the square root of the conditional variance, and n_{z_c} is the number of simulated scenarios where Z es ≥ Z_c .

3. RESULTS

The cumulative curves of metal quantity and probability versus nickel cut-off values, the relative frequency histograms, and the contact plots between weathering crust horizons are presented in Figures 1, 2, and 3.

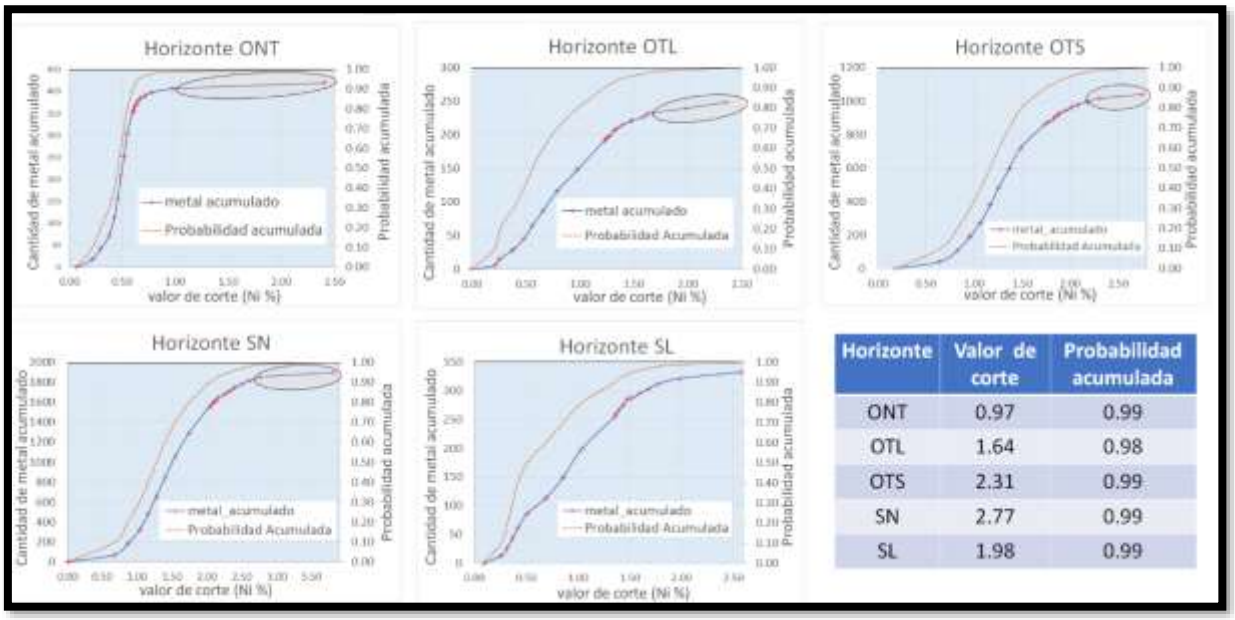

Horizonte	Valor de corte	Probabilidad acumulada
ONT	0.97	0.99
OTL	1.64	0.98
OTS	2.31	0.99
SN	2.77	0.99
SL	1.98	0.99

Figure 1. Graphs of cumulative curves of metal quantity and probability versus nickel cut-off values.

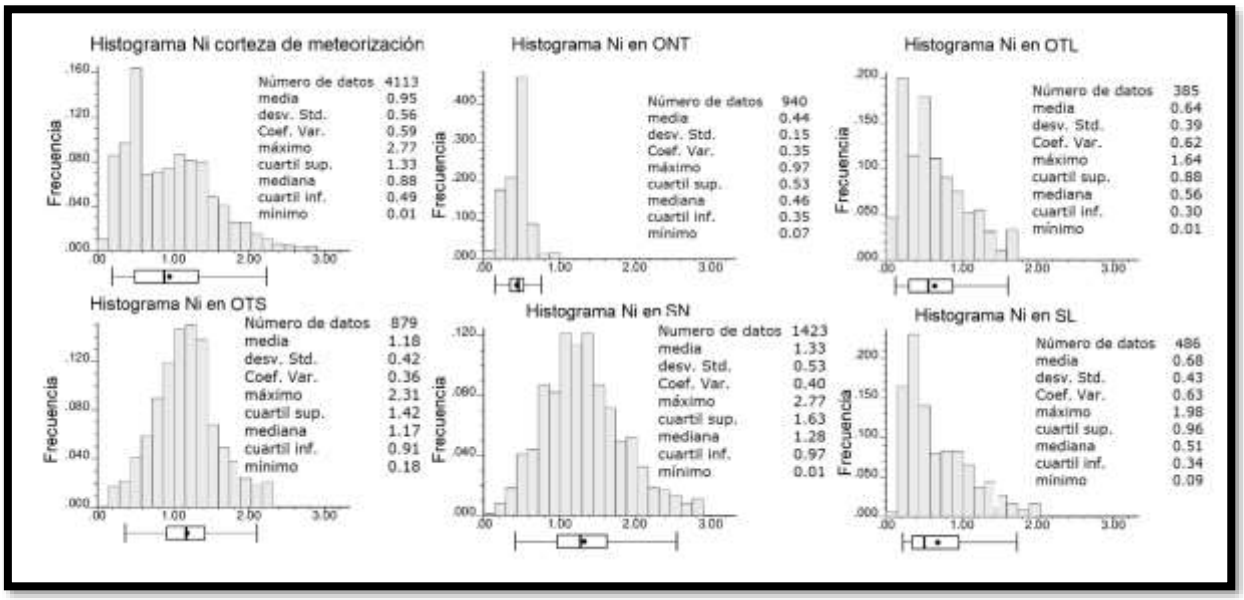

Figure 2. Relative frequency histograms for the weathering crust and its horizons, with their respective "Box and Whisker" plots

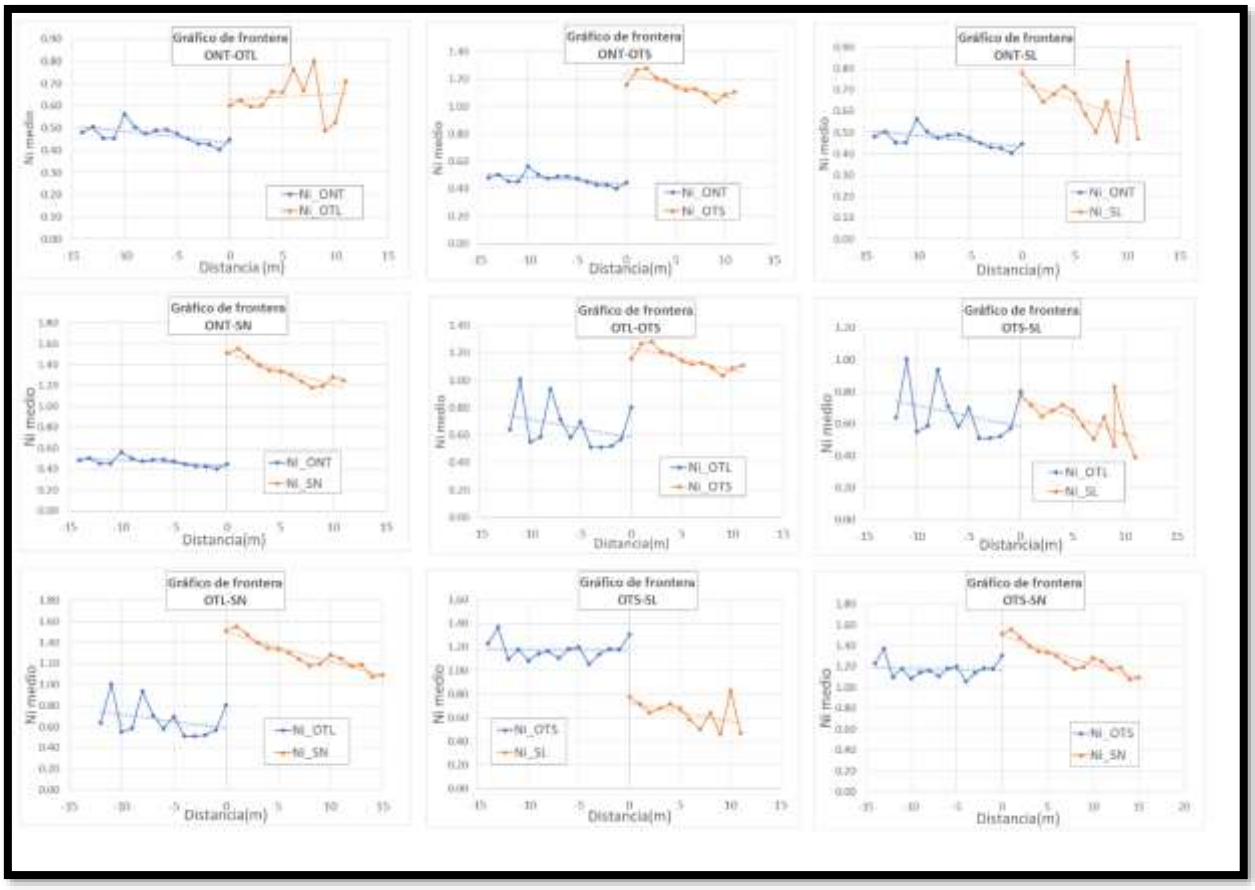

Figure 2. Contact plots between weathering crust horizons.

The structural function fitted (equation 11) to the global Gaussian semi-variograms of nickel (Figure 4) within the limits of the study sector is presented below:

$$\gamma(h_{x,y,z}) = 0.10 + 0.5 \cdot Esf(1) \cdot \left[\frac{h_{1,1}}{56m}, \frac{h_{2,1}}{56m}, \frac{h_{3,1}}{10m}\right] + 0.40 \cdot Exp(2) \cdot \left[\frac{h_{1,2}}{143.5m}, \frac{h_{2,2}}{143.5m}, \frac{h_{3,2}}{7m}\right] \quad (11)$$

Sequential Gaussian Simulation was performed in the SGeMS geostatistical software using the SGSIM algorithm (Remy et al., 2011). In total, the nickel value was simulated at 233,100 locations (nodes), with 74 nodes in the X direction, 94 in the Y direction, and 35 in the Z direction, covering the three-dimensional space within the limits of the weathering crust of the sector under study. Figures 5, 6, and 7 show the results of the simulation validation process.

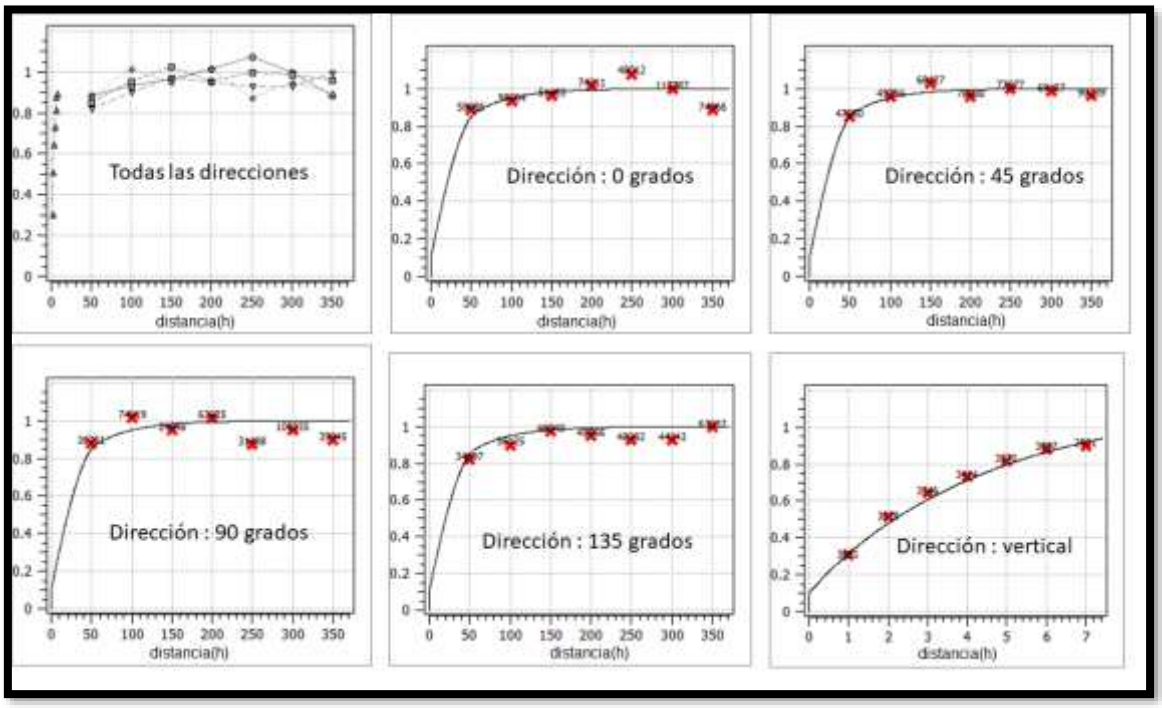

Figure 3. Directional experimental Gaussian semi-variograms of nickel according to directions 0º (Dir=0), 45º (Dir=45), 90º (Dir=90), 135º (Dir=135), and vertical (downhole) with fitted horizontal and vertical theoretical model.

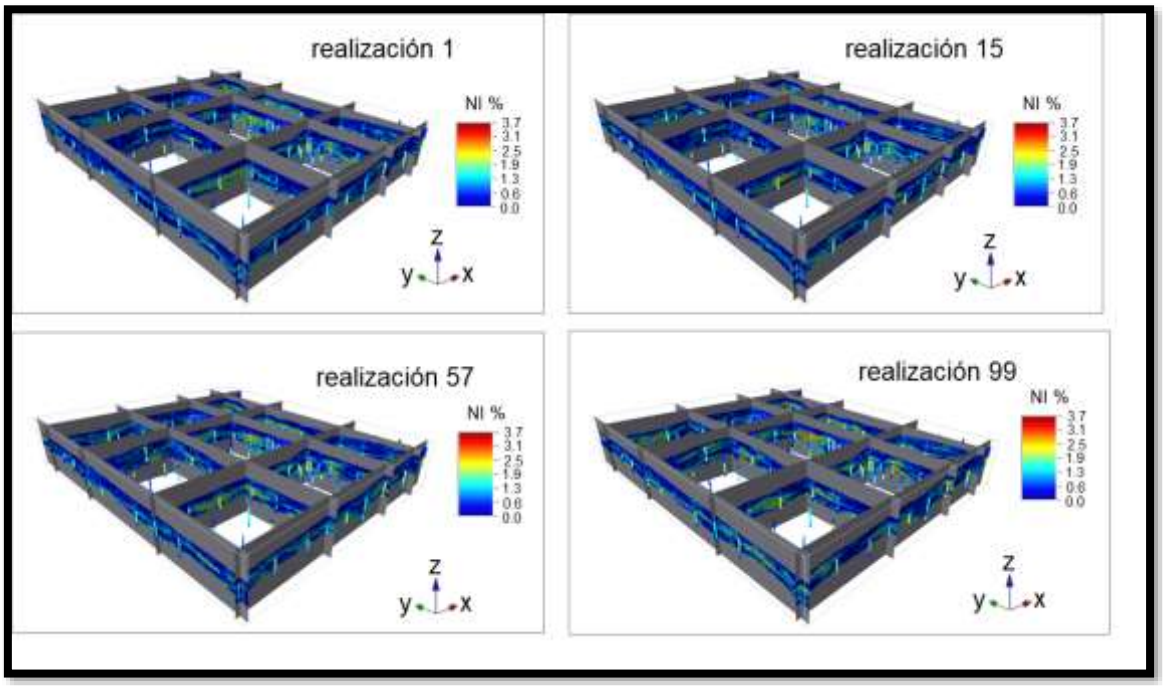

Figure 4. Perspective view of realizations 1, 15, 57, and 99 of simulated nickel values versus real data (composites).

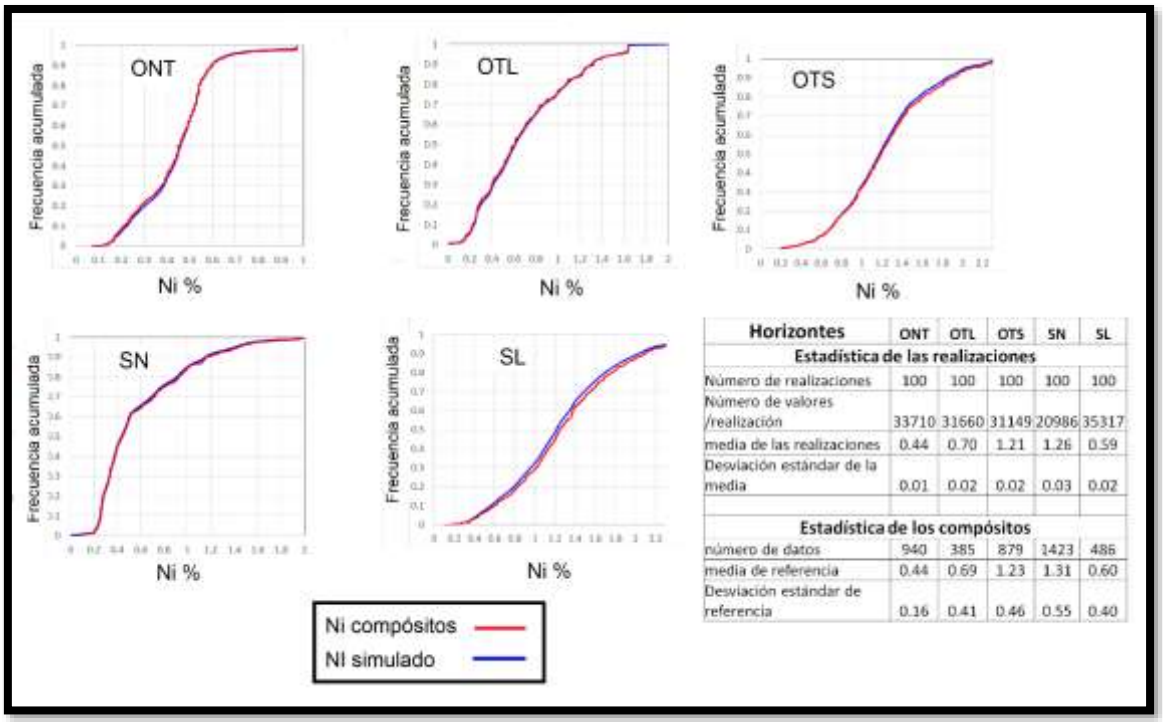

Horizontes	ONT	OTL	OTS	SN	SL
Estadística de las realizaciones					
Número de realizaciones	100	100	100	100	100
Número de valores /realización	33710	31660	31149	20986	35317
media de las realizaciones	0.44	0.70	1.21	1.26	0.59
Desviación estándar de la media	0.01	0.02	0.02	0.03	0.02
Estadística de los compósitos					
número de datos	940	385	879	1423	486
media de referencia	0.44	0.69	1.23	1.31	0.60
Desviación estándar de referencia	0.16	0.41	0.46	0.55	0.40

Figure 5. Cumulative frequency curves and corresponding average statistics of real and simulated nickel values, by lithological weathering horizons.

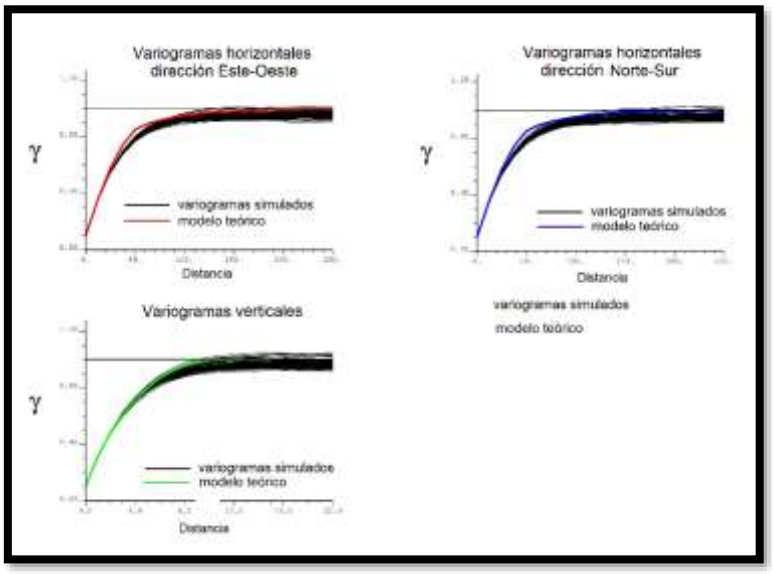

Figure 6. Simulated global Gaussian semi-variograms versus fitted theoretical model (100 equiprobable scenarios).

As a result of calculating the estimated mineral probability values, the following mineral probability classes were established:

- **High probability:** panels with a probability value greater than or equal to 0.8.
- **Medium probability:** panels with probability values between 0.5 and 0.8.
- **Low probability:** panels with probability values between 0.01 and less than 0.5.
- **Non-mineral:** panels whose nickel grade was lower than the cut-off grade for the 100 simulated equiprobable scenarios.

Based on the preceding classification, the mineral probability model was created in 25 m x 25 m x 1 m panels (Figure 8). Using the mean values obtained for tonnage, metal quantity, nickel grade, and confidence intervals appearing in Table 2, the graphs in Figures 9, 10, and 11 were elaborated.

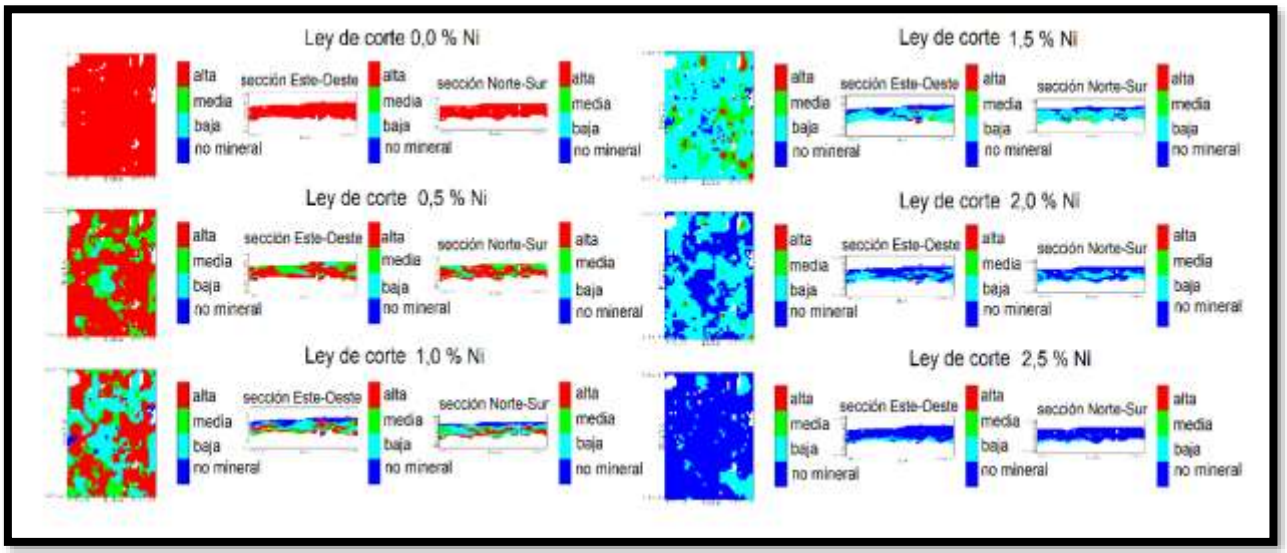

Figure 7. Average mineral probability viewed through sections and levels according to probability classes established in accordance with nickel cut-off values, in 25 m x 25 m x 1 m panels for 100 equiprobable scenarios.

Table 1. Recursos recuperables para el tonelaje, la cantidad de metal y la ley media de níquel con sus respectivos errores medios globales e intervalos de confianza asociados

Parameter	Ley de corte Ni (%)	Error medio global	valor Medio del parámetro	valor medio - IC 95%	valor medio + IC 95%
Tonnage	0.0	0	737	737	737
	0.5	37	515	479	552
	1.0	39	359	320	398
	1.5	54	257	202	311
	2.0	48	219	170	267
	2.5	59	195	136	254
Metal Quantity (t x % Ni)	0.0	35	550	514	585
	0.5	46	502	455	548
	1.0	63	499	436	562
	1.5	105	456	351	561
	2.0	120	484	364	604
	2.5	173	516	344	689
Ni Grade	0.0	0.05	0.78	0.74	0.83

(%)	0.5	0.05	0.93	0.88	0.98
	1.0	0.06	1.33	1.27	1.39
	1.5	0.08	1.75	1.66	1.83
	2.0	0.10	2.20	2.10	2.31
	2.5	0.12	2.64	2.52	2.76

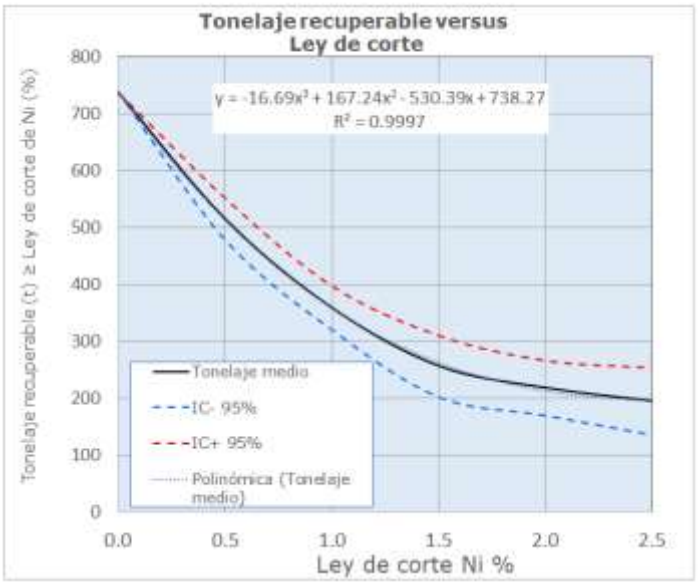

Figure 8. Curves of recoverable tonnage and confidence intervals versus nickel cut off grade in 25 m x 25 m x 1 m panel.

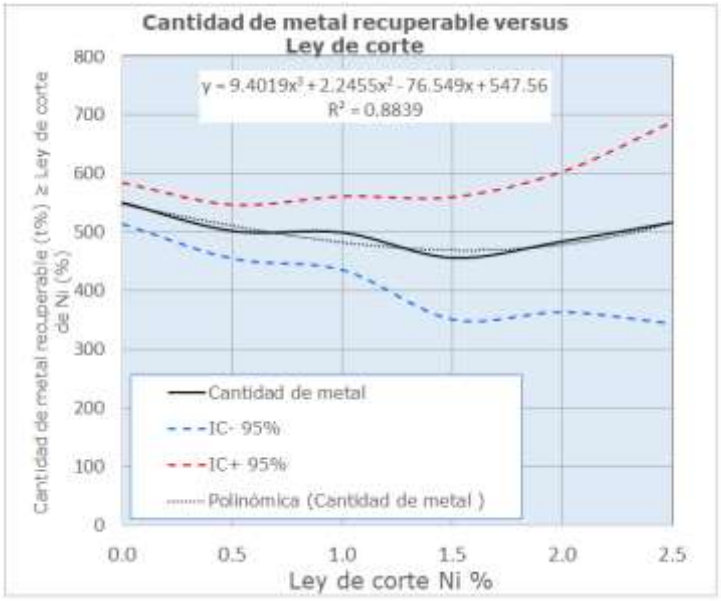

Figure 9. Curves of recoverable metal quantity and confidence intervals versus nickel cut-off grade in 25 m x 25 m x 1 m panel.

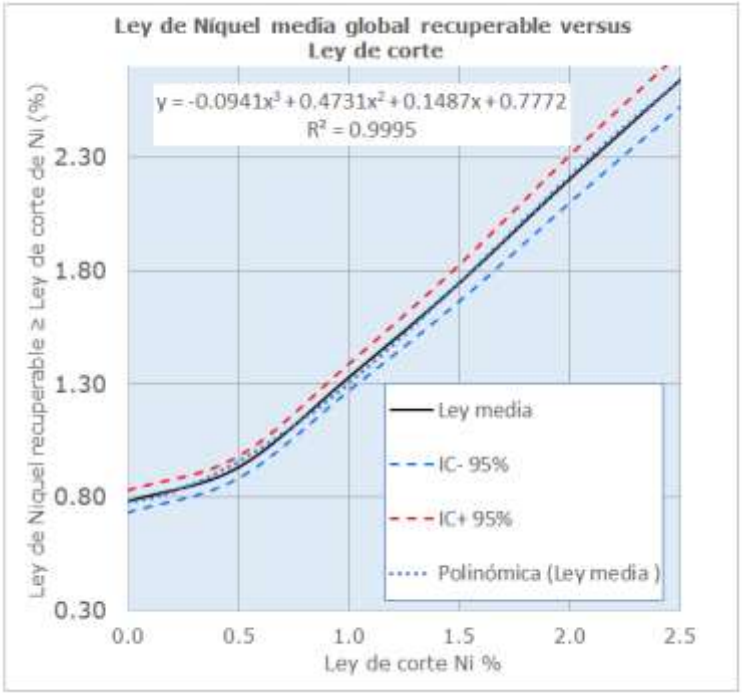

Figure 10. Curves of recoverable mean nickel grade and confidence intervals in 25 m x 25 m x 1 m panel versus nickel cut-off grade.

4. DISCUSSION

The capping of nickel values for the five lithological weathering horizons allowed for the establishment of cut-off values based on the criterion of slope change and the spacing of points in the graph above 98% probability (Figure 1).

Globally, nickel values possess a multimodal statistical distribution—specifically, the nickel histogram for the entire weathering crust is bimodal (Figure 2)—with positive skewness. This suggests a mixture of two or more populations, exhibiting two relative frequency maxima: one associated with low nickel values ($\approx$ 0.5%) and the other with medium values ($\approx$ 1.0%). When nickel values are analyzed by weathering horizons, frequency distributions in ONT, OTS, and SN appear more symmetric. This is not the case for nickel in the OTL and SL horizons, where positive skewness is more evident, with box-and-whisker plots showing a separation between the mean and median, as well as a decrease in class frequency towards high values.

The analysis of boundary plots (Figure 3) shows that the boundaries between lithological weathering horizons are hard in all cases; there is no transition in nickel content when crossing the borders between them, and therefore, they are interpreted as different domains.

The structural analysis performed via calculated experimental semi-variograms (Figure 4) evidences the existence of spatial continuity, both in the plane of the lithological weathering horizons and across them. Isotropy exists in the plane of the lithological weathering horizons, given that the fitted ranges are similar. The range in the vertical direction is smaller, evidencing a faster transition through that direction.

Cross-validation showed that the fitted theoretical model achieves an acceptable degree of predictability, as the mean error between real and estimated values approaches zero (0.01) and the linear correlation coefficient is 0.75.

Gaussian simulation successfully reproduced the textural characteristics of the nickeliferous mineralization, establishing a good spatial correspondence of the simulated variable values with the composites used for simulation (Figure 5). From a statistical point of view, both the mean values obtained and the cumulative frequency curves for nickel of the reference distribution (composites) and the simulated nickel according to lithological weathering horizons (Figure 6) are approximately similar, indicating that the statistics are satisfactorily reproduced. The simulated directional Gaussian semi-variograms possess the same shape and ranges as the theoretical curves fitted to the composites (Figure 7).

According to the classification adopted based on the mean mineral probability values obtained for each 25 m x 25 m x 1 m panel, the highest recoverable mineral probability is reached for nickel cut-off grade values less than or equal to 1% nickel (Figure 8). For values higher than this, there is a predominance of panels with mineral probability values below 0.50, evidencing an appreciable decrease in the degree of confidence and continuity of nickeliferous mineralization starting from the 1.0% nickel cut-off value. An optimal recoverable mineral probability value would be obtained for a nickel cut-off grade located between the cut-off values of 1.0% - 1.5% nickel.

As the nickel cut-off value increases, the estimated mineral probability of recoverable resources decreases. When a nickel cut-off value equal to 0% is used, the recoverable mineral probability is maximized, with an almost absolute predominance of panels with high mineral probability, since all panels are considered recoverable resources. When the nickel cut-off grade is equal to 2.5%, the probability of recoverable resources is minimized, with a predominance of non-mineral panels. The medium scenario of recoverable mineral probability is reached when the cut-off grade is equal to 1.0% nickel.

Above, in Table 2, the estimated figures of global recoverable resources obtained by cut-off grades are presented, calculated with a 95% probability

significance level for a panel of dimensions 25 m x 25 m x 1 m. According to the obtained figures, the recoverable mineral tonnage for the panel ranges between 195 metric tonnes (t) and 737 t, with an error between 0 t and 59 t. For metal quantity, the mean values obtained range between 516 t and 550 t per percent of nickel, with an error between 35 t and 173 t per percent. Meanwhile, for the mean nickel grade, nickel values were estimated between 0.46% and 3.16%, with errors between 0.05% and 0.12%.

As observed in the graphs of Figures 9, 10, and 11, the uncertainty of recoverable tonnage, metal quantity, and mean grade gradually increases from the 0% nickel cut-off value to the 2.5% nickel cut-off value. Judging by the increase in the width of the confidence intervals obtained from the computed mean errors, this is due to the drastic decrease in the number of panels with simulated high grades (equal to or greater than 1.5% nickel). This influences the increase of Student's t probability values in the error calculation, as a consequence of the low proportion of composites with high grades used as primary data in the simulation process. All this implies a high risk with a negative impact on mining.

The polynomial fit performed on the experimental curves of recoverable tonnage, metal quantity, and mean grade is significant, given the obtained coefficient of determination (R^2) values exceed 0.88 in all cases. This means that the fitted models sufficiently explain the variation of estimated parameters, which is useful for making predictions for other nickel cut-off grade values.

Previously, global deterministic estimates were made in the San Felipe deposit by non-linear estimation methods to determine recoverable resources. First by Rodríguez et al. (2001) and subsequently by Horton and Lipton (2002); these latter authors recommended utilizing geostatistical conditional simulation in one or several areas of the deposit to study the relationships between those selective mining units, the mining method, and the production rate.

Therefore, the methodology and results of this research constitute a novelty in the application of geostatistical conditional simulation to the determination of recoverable resource potential in the San Felipe deposit.

5. CONCLUSIONS

- The application of Sequential Gaussian Simulation (SGS) with change of support proves to be effective for predicting recoverable resources in the San Felipe deposit, faithfully reproducing the statistics (histograms), spatial continuity (variograms), and geological

heterogeneity of the nickeliferous mineralization. The 100 equiprobable scenarios allowed for the quantification of uncertainty, an advancement over previous studies based on traditional deterministic estimation.

- Varying the cut-off grade on a specific estimation support produces an effect on recoverable resources: as the cut-off grade increases, tonnage decreases; the contrary occurs with the mean nickel grade, which increases. However, probabilistic uncertainty increases; therefore:

- The cut-off grade directly impacts mining parameters; by increasing it, tonnage decreases because only high-grade blocks are selected, while the mean grade grows due to the statistical truncation effect. However, uncertainty amplifies at high grades (>1.5% Ni) due to lower data density and geological heterogeneity.

- Recoverable tonnage and metal decrease as the cut-off grade increases (from 737 t to 195 t and from 550 t·% to 516 t·% for cut-offs of 0% to 2.5% Ni, respectively). The mean grade increases (from 0.78% Ni to 2.64% Ni), but with greater uncertainty (mean error grows from ±0.05% to ±0.12% Ni). This reflects the scarcity of high-grade data and the required selectivity.

- Therefore, to maximize economic benefit, we recommend a cut-off grade between 1.0% and 1.5% Ni, where recoverable tonnage, mean grade, and operational risk are balanced, given the obtained uncertainty.

- We consider that the results achieved could be improved with a higher level of geological information. The density of the current exploration grid in the case study sector and in prospective zones of the San Felipe deposit is 100 m x 100 m, which is insufficient to capture the structures of nickeliferous mineralization and grade variability at a small scale, preventing the acquisition of recoverable resources with a higher degree of certainty at a local scale. It is recommended to increase the density of the exploration grid, especially in less densely drilled zones.

- Future studies should be conducted to incorporate semi-variogram information by horizon (not just global) to refine the simulation. The results obtained define the resources that can be recovered in the sector under investigation at the time of mining exploitation. The methodology developed in this work is transferable to other lateritic

deposits with similar geological characteristics, so we recommend its future use.

6. ACKNOWLEDGMENTS

The authors wish to thank Commercial Caribbean Nickel S.A., concessionaire of the San Felipe Nickel deposit, for allowing us to use the corresponding information of the case study area for the realization of this work, and the National Office of Mineral Resources for the support provided to bring its publication to a successful conclusion.

6. REFERENCES

Artica, C. (2023). Comparison of two quantitative mineral resource classification methods – a case study from a large copper porphyry-skarn deposit. *Mineral Resource Estimation Conference 2023*. Perth, Australia: The Australasian Institute of Mining and Metallurgy, pp. 166-178. Publication Series No 2/2023, ISBN 978-1-922395-14-6. Consultado: 17/02/2025. Disponible en: https://www.ausimm.com/publications/conference-proceedings/mineral-resource-estimation-conference-proceedings-2023/comparison-of-two-quantitative-mineral-resource-classification-methods--a-case-study-from-a-large-copper-porphyry-skarn-deposit/

Chang-Rodríguez, A. y Rojas-Purón, A. L. (2018). Movilidad geoquímica y grado de meteorización del yacimiento San Felipe, Camagüey, Cuba. *Minería y Geología*, *34*(2), 122-135. Consultado: 17/02/2025. Disponible en: https://www.redalyc.org/journal/2235/223554994001/html/

Chica-Olmo, M. (1987). *Análisis Geoestadístico en el Estudio de la Explotación de Recursos Minerales*. (Tesis doctoral, España).

Cobas-Botey, R. M. (2017). *Modelo geológico descriptivo de las lateritas ferroniquelíferas del depósito San Felipe, Camagüey, Cuba*. (Tesis doctoral, Universidad de Moa).

Cobas-Botey, R. M., Formell-Cortina, F. Y., Leyva-Rodríguez, C. A. (2017). Modelo geológico descriptivo del yacimiento laterítico San Felipe, Camaguey, Cuba. *Minería y Geología*, *33*(3), 251-265. Consultado: 17/02/2024. Disponible en: https://www.redalyc.org/journal/2235/223551846001/html/

Deutsch, C. V. y Journel, A. G. (1998). *GSLIB: Geostatistical Software Library and User's Guide*. S.l.: Oxford University Press. Applied

geostatistics series, ISBN 978-0-19-510015-0. Consultado: 17/02/2025. Disponible en: https://books.google.com.cu/books?id=CNd6QgAACAAJ.

Gallardo, T., Chang, A., Tauler, E. Y Proenza, J. (2010). El yacimiento de San Felipe (Camagüey, Cuba): un ejemplo de lateritas niquelíferas tipo arcilla. *Macla*, *13*, 87-88.

Kapageridis, I., Apostolikas, A. Y., Kamaris, G. (2021). Contact Profile Analysis of Resource Estimation Domains: A Case Study on a Laterite Nickel Deposit. *Materials Proceedings*, *5*(1), 89. Consultado: 26/05/2025. Disponible en: https://www.mdpi.com/2673-4605/5/1/89.

Murphy, M., Parker, H., Ross, A. y AUDET, M. A. (2005). Ore-Thickness and Nickel Grade Resource Confidence at the Koniambo Nickel Laterite (A Conditional Simulation Voyage of Discovery). En: O. Leuangthong y C. V. Deutsch (eds.), *Geostatistics Banff 2004*. Dordrecht: Springer Netherlands, pp. 469-478. ISBN 978-1-4020-3610-1. Consultado: 17/02/2025. Disponible en: https://doi.org/10.1007/978-1-4020-3610-1_47.

Neufeld, C. y Leuangthong, O. (2005). The Calculation of Recoverable Reserves. Centre for Computational Geostatistics Department of Civil and Environmental Engineering University of Alberta, no. 301. Consultado: 26/05/2025. Disponible en: https://www.ccgalberta.com/ccgresources/report07/2005-301-recoverable_reserves.pdf.

Remy, N., Boucher, A. y Wu, J. (2009). Applied Geostatistics with SGeMS: A User's Guide. *Mathematical Geosciences*, *41*(3), 353-356. ISSN 1874-8953. DOI 10.1007/s11004-009-9217-5.

Remy, N., Boucher, A., Wu, J., Ting, L., Maharaja, A. y Gupta, R. (2011). *SGeMS*. C++. 1 septiembre 2011. S.l.: Advanced Resources & Risk Technology, LLC. Consultado: 26/05/2025. Disponible en: http://www.ar2tech.com.

Richmond, A. (2013). Conditional Simulation of a Nickel Laterite Deposit using Unfolding. *APCOM 2013*. S.l.: s.n., pp. 6. Consultado: 17/02/2024. Disponible en: https://martlet.com.au/wp-content/uploads/2020/08/2013_APCOM_Richmond_Conditional_Simulation_of_nickel_laterite_deposit_using_unfolding.pdf.

Rodríguez, C., Rivers, C., Parianos, J., Mwasinga, P., Potter, S. y Coombes, J. (2001). Mineral Resource Estimate of the San Felipe deposit. Technical Report. S.l.: bhpbillinton. 1966/009633/06. ONRM.

Rodríguez-Catalá, A. y Rodríguez-Infante, A. (2021). Sistema de fallas del yacimiento laterítico niquelífero San Felipe, Camagüey, Cuba. *Minería y Geología*, *37*(2), 162-180. ISSN 1993-8012. Consultado: 28/02/2024. Disponible en: http://scielo.sld.cu/scielo.php?script=sci_abstract&pid=S1993-80122021000200162&lng=es&nrm=iso&tlng=es.

Rossi, M. E. y Deutsch, C. (2014). *Mineral Resource Estimation*. Springer Dordrecht Heidelberg New York London. ISBN 978-1-4020-5716-8. Consultado: 26/05/2025. Disponible en: www.springer.com.

Sinclair, A. J., & Blackwell, G. H. (2006). *Applied mineral inventory estimation*. Cambridge University Press.

Sterk, R., De Jong, K., Partington, G., Kerkvliet, S. y Van De Ven, M. (2019). Domaining in Mineral Resource Estimation: A Stock-Take of 2019 Common Practice. *Kenex*. 25 noviembre 2019. pp. 13. Consultado: 19/02/2025. Disponible en: https://kenex.com.au/company/publications/.

Webster, R. y Oliver, M. A. (2007). Cross-Validation. *Geostatistics for Environmental Scientists*. Second Edition. John Wiley & Sons. ISBN 978-0-470-02858-2. Consultado: 19/02/2025. Disponible en: www.wiley.com.

Yamamoto, J. K. (1999). Quantification of uncertainty in ore-reserve estimation: Applications to Chapada copper deposit, State of Goiás, Brazil. *Natural Resources Research*, *8*(2), 153-163.

Adicional Information

Conflict of interest

The authors declare that there are no conflicts of interest.

Authors Contribution

JAAT: Conceptualization and geostatistical processing, main drafter of the manuscript. ACP: Supervisor, research design, final drafting. EEC: Supervisor, research design; reviewer of processing and co-drafter of geostatistical information and of figures, charts, and tables. RMCB: Co-drafter of the geological part of the "San Felipe" deposit, revision of terminology employed.

ORCID

JAAT, https://orcid.org/0000-0001-6879-4626

ACP, https://orcid.org/0000-0002-6841-8086

EEC, https://orcid.org/0000-0001-7311-8382

RMCB, https://orcid.org/0009-0004-1178-3781

Received:29/05/2025

Accepted:15/07/2025